On geometric control models of a robotic snake

Aleš Návrat and Petr Vašík[i]

Brno University of Technology, Faculty of Mechanical Engineering
Institute of Mathematics
Technická 2896/2, 616 69 Brno
Czech Republic
`navrat.a@fme.vutbr.cz, vasik@fme.vutbr.cz`

Abstract. We present three possible ways of controlling a robotic system called a 3–link snake robot. First, we recall the classical approach by constructing the controlling vector fields and their Lie brackets. Next we modify the coordinate system in order to obtain a nilpotent approximation of the controlling distribution. This is based on the notions of sub–Riemannian geometry. The third model is based on serpenoid curve and maintains the global control task.

Keywords: robotic snake, local control

MSC 2010 classification: 93B27

1   Introduction

Within this paper, we consider a 3–link snake robot moving on a planar surface. More precisely, it is a model when to each link a pair of wheels is attached and the joints of the legs are motorised and thus the possible motion directions are determined. Local controllability of such mechanism is known, see [5]. If the generalized coordinates are considered, the non–holonomic forward kinematic equations can be understood as a Pfaff system and thus a distribution on the configuration space is given. Rachevsky–Chow Theorem implies that the appropriate non–holonomic system is locally controllable if the corresponding distribution is not integrable and the span of the Lie algebra generated by the controlling distribution is of the same dimension as the configuration space. The spanned Lie algebra is then naturally endowed by a filtration which shows the way to realize the motions by means of the vector field brackets. In our case, the system is locally controllable and the appropriate filtration growth vector is $(2, 3, 5)$. The above considerations follow the geometric control ideas which is a

---
[ii]

modern geometrical approach to the control theory. For further applications of differential geometry in robotics see e.g. [7].

Note that to compose a motion control algorithm, the Lie bracket motions have to be considered to restore the initial position and allow the repetition of propulsion. As the Lie bracket motions are realized by means of so–called periodic input, an error occurs. To classify the model error, we establish so–called nilpotent approximation of the controlling distribution in which, according to [6], the periodic input models the Lie bracket motions that are accurate up to the second order. Furthermore, in e.g. [4], a convenient error estimates in the nilpotent approximation are described. Note that all constructions are local in the neighbourhood of 0 and the constructed nilpotent approximation is referred to as homogeneous.

2 Preliminaries

We recall the following concepts of functions or vector fields orders and distribution weights, see [4]. Let $X_1, ..., X_m$ denote the smooth vector fields on a manifold M and $C^\infty(p)$ denote the set of germs of smooth functions at $p \in M$. For $f \in C^\infty(p)$ we say that the Lie derivatives $X_i f, X_i X_j f, ...$ are non–holonomic derivatives of f of order 1,2,... The non–holonomic derivative of order 0 of f at p is $f(p)$.

Definition 1. Let $f \in C^\infty(p)$. Then the non–holonomic order of f at p, denoted by $\mathrm{ord}_p(f)$, is the biggest integer k such that all non–holonomic derivatives of f of order smaller than k vanish at p.

Note that in case $M = \mathbb{R}^n$, $m = n$ and $X_i = \partial_{x_i}$, for a smooth function f, $\mathrm{ord}_0(f)$ is the smallest degree of monomials having nonzero coefficient in the Taylor series. In the language of non–holonomic derivatives, the order of a smooth function is given by the formula, [4]:

$$\mathrm{ord}_p(f) = \min\left\{ s \in \mathbb{N} : \exists i_1, ..., i_s \in \{1, ..., m\} \text{ s.t. } (X_{i_1} \cdots X_{i_s} f)(p) \neq 0 \right\},$$

where the convention reads that $\min \emptyset = \infty$.

If we denote by $\mathrm{VF}(p)$ the set of germs of smooth vector fields at $p \in M$, the notion of non–holonomic order extends to the vector fields as follows:

Definition 2. Let $X \in \mathrm{VF}(p)$. The non–holonomic order of X at p, denoted by $\mathrm{ord}_p(X)$, is a real number defined by:

$$\mathrm{ord}_p(X) = \sup\left\{ \sigma \in \mathbb{R} : \mathrm{ord}_p(Xf) \geq \sigma + \mathrm{ord}_p(f), \forall f \in C^\infty(p) \right\}.$$

Note that $\operatorname{ord}_p(X) \in \mathbb{Z}$. Moreover, the null vector field $X \equiv 0$ has infinite order, $\operatorname{ord}_p(0) = \infty$. Furthermore, $X_1, ..., X_m$ are of order ≥ -1, $[X_i, X_j]$ of order ≥ -2, etc. Using the notion of a vector field order one can define

Definition 3. A family of m vector fields $(\hat{X}_1, ..., \hat{X}_m)$ defined near p is called a first order approximation of $(X_1, ..., X_m)$ at p if the vector fields $X_i - \hat{X}_i, i = 1, ..., m$ are of order ≥ 0 at p.

Finally, to define the weights of distributions we use the same notation as in [4]. Let us by Δ^1 denote the distribution $\Delta^1 = \operatorname{span}\{X_1, ..., X_m\}$ and for $s \geq 1$ define $\Delta^{s+1} = \Delta^s + [\Delta^1, \Delta^s]$, where $[\Delta^1, \Delta^s] = \operatorname{span}\{[X, Y] : X \in \Delta^1, Y \in \Delta^s\}$. Then $\Delta^s = \operatorname{span}\{X_I : |I| \leq s\}$. Note that this directly leads to the fact that every $X \in \Delta^s$ is of order $\geq -s$. Now let us consider the sequence $\Delta^1(p) \subset \Delta^2(p) \subset \cdots \subset \Delta^{r-1} \subsetneq \Delta^r(p) = T_p M$, where $r = r(p)$ is called the degree of non–holonomy at p. Set $n_i(p) = \dim \Delta^i(p)$. Then we can define the weights at p, $w_i = w_i(p), i = 1, ..., n = n_{r(p)}$ by setting $w_j = s$ if $n_{s-1}(p) < j \leq n_s(p)$, where $n_0 = 0$. In other words, we have

$$w_1 = \cdots = w_{n_1} = 1, \ w_{n_1+1} = \cdots = w_{n_2} = 2, ..., w_{n_{r-1}+1} = \cdots = w_{n_r} = r.$$

The weights at p form an increasing sequence $w_1(p) \leq \cdots \leq w_n(p)$.
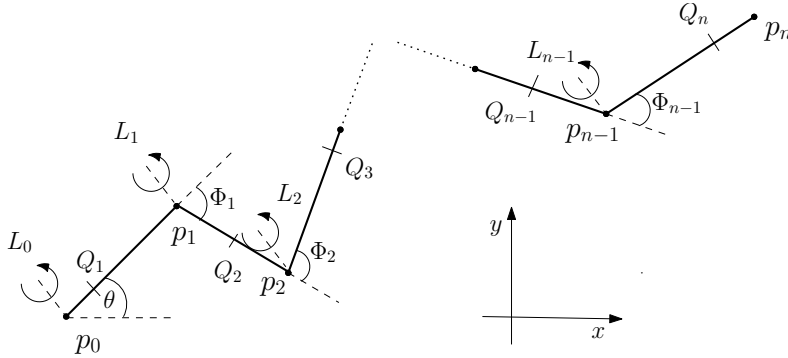
3   3–link snake robot

Figure 1. Snake robot model

The snake robot model is generally composed of n links of the lengths $l_i, \ i = 1, .., n$, interconnected by $(n - 1)$ motorised joints with the axis of rotation denoted by $L_i, \ i = 1, .., n - 1$, and each link is endowed with a pair of passive wheels at arbitrary position within the appropriate link $Q_i, \ i = 1, .., n - 1$, see Figure 1. To describe such a complex model, it is suitable to use the tools of

Conformal Geometric Algebra (CGA), where all the model modification can be carried on quite easily, see [1]. For the case of a 3–link snake in CGA see [2].

The snake robot described in this paper consists of 3 rigid links of constant length 2 interconnected by 2 motorized joints. To each line, in the centre of its mass, a pair of wheels is attached to provide an important snake-like property that the ground friction in the direction perpendicular to the link is considerably higher than the friction of a simple forward move. In particular, this prevents the slipping sideways. To describe the actual position of a snake robot we need the set of 5 generalized coordinates $q = (x, y, \theta, \Phi_1, \Phi_2)$ which describe the configuration of the snake robot as shown in Figure 2 and forms a manifold M as a phase space.
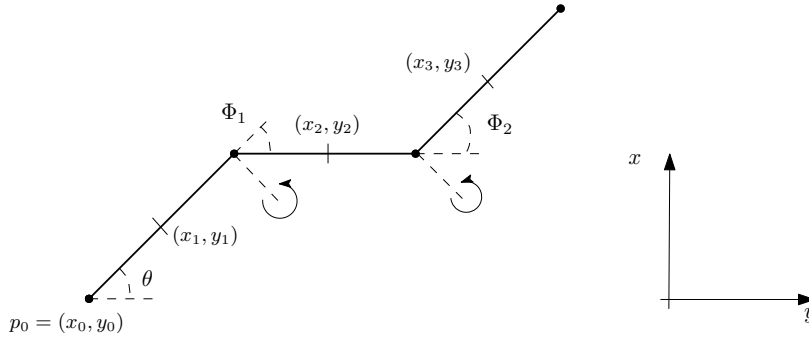

Figure 2. 3–link snake robot model

Note that the forward kinematics is calculated w.r.t. the head point (x_0, y_0) and the parameterization by $\dot{x}$ and $\dot{y}$. The non–singular positions then form a 2–dimensional distribution which can be determined by the vector fields X, Y e.g. with the following coordinates:

$$
\begin{aligned}
X_1 =& 1 \\
X_2 =& 0 \\
X_3 =& 2\sin(\theta) \\
X_4 =& -4\sin(\theta)\sin(\Phi_1 + \pi/6) - 2\sin(\theta) - 2\cos(\theta + \Phi_1 + \pi/6) \\
X_5 =& 8\cos(\Phi_2 + \pi/3)\sin(\Phi_1 + \pi/6)\sin(\theta) - 4\sin(\theta)\cos(\Phi_1 + \Phi_2) \\
& + 4\cos(\Phi_2 + \pi/3)\cos(\theta + \Phi_1 + \pi/6) + 4\sin(\theta)\sin(\Phi_1 + \pi/6) \\
& + 2\cos(\theta + \Phi_1 + \pi/6) + 2\sin(\theta + \Phi_1 + \Phi_2)
\end{aligned}
\tag{1}
$$

and

$$
\begin{aligned}
Y_1 =&\, 0 \\
Y_2 =&\, 1 \\
Y_3 =& -2\cos(\theta) \\
Y_4 =&\, 4\cos(\theta)\sin(\Phi_1 + \pi/6) + 2\cos(\theta) - 2\sin(\theta + \Phi_1 + \pi/6) \qquad (2) \\
Y_5 =& -8\cos(\Phi_2 + \pi/3)\sin(\Phi_1 + \pi/6)\cos(\theta) + 4\cos(\theta)\cos(\Phi_1 + \Phi_2) \\
& + 4\cos(\Phi_2 + \pi/3)\sin(\theta + \Phi_1 + \pi/6) - 4\cos(\theta)\sin(\Phi_1 + \pi/6) \\
& + 2\sin(\theta + \Phi_1 + \pi/6) - 2\cos(\theta + \Phi_1 + \Phi_2)
\end{aligned}
$$

and their Lie bracket $[X, Y]$ and two higher order brackets $[[X, Y], X]$ and $[[X, Y], Y]$. Evaluating these vector fields at the point $init = (0, 0, 0, -\frac{\pi}{3}, \frac{\pi}{3})$ which is considered in the following as the snake's initial position, we obtain

$$
\begin{aligned}
X(init) =&\, (1, 0, 0, -\sqrt{3}, 2\sqrt{3}), \\
Y(init) =&\, (0, 1, -2, 3, 0), \\
[X, Y](init) =&\, (0, 0, 4, -12, 12), \\
[[X, Y], X](init) =&\, (0, 0, 8, -36, 60), \\
[[X, Y], Y](init) =&\, (0, 0, 0, -4\sqrt{3}, 20\sqrt{3}).
\end{aligned}
$$

The motion planning is then modelled sequentially, meaning that e.g. the motion in the direction of the x axis from the initial position and consequent transformation into the shifted initial position (i.e. only the x coordinate is different) again is formed by the linear combination

$$
(1, 0, 0, 0, 0) \propto (576 + 360\sqrt{3})X - 22[X, Y] + 11[[X, Y], X] - 101\sqrt{3}[[X, Y], Y],
$$

where the Lie bracket motions are realized by so–called periodic input in the form

$$
u(t) = (-A\omega\sin\omega t, A\omega\cos\omega t) \qquad (3)
$$

with suitable choice of $A \in \mathbb{R}$ sufficiently small amplitude and $\omega \in \mathbb{R}$. For further details about the precise form of inputs for composed Lie brackets see [6].

4 Nilpotent Approximation

We proceed according to Bellaïche's algorithm, see e.g. [4]. We shall use the following notation: $(x_1, x_2, x_3, x_4, x_5) := (x, y, \theta, \Phi_1, \Phi_2)$ and the resulting privileged coordinates will be denoted by $(z_1, z_2, z_3, z_4, z_5)$. We recall the definition of privileged coordinates, [4], taking into account the notation from Section 2.

Definition 4. A system of privileged coordinates at p is a system of local coordinates $(y_1, ..., y_n)$ such that $\mathrm{ord}_p(y_j) = w_j$ for $j = 1, ..., n$.

Yet, note that the algorithm starts with the coordinate transformation into $(y_1, y_2, y_3, y_4, y_5)$ such that $\partial_{y_1} = X$, $\partial_{y_2} = Y$, $\partial_{y_3} = [X,Y]$, $\partial_{y_4} = [[X,Y],X]$ and $\partial_{y_5} = [[X,Y],Y]$. The transformation matrix at 0 is of the form

$$
\begin{pmatrix}
1 & 0 & 0 & 0 & 0 \\
0 & 1 & 0 & 0 & 0 \\
1/4\sqrt{3} & 5/4 & 5/4 & 5/12 & 1/12 \\
-1/8\sqrt{3} & -3/8 & -1/2 & -5/24 & -1/24 \\
1/8 & 1/8\sqrt{3} & 1/4\sqrt{3} & 1/8\sqrt{3} & 1/24\sqrt{3}
\end{pmatrix}.
$$

If the controlling vector fields are denoted as

$$
\begin{aligned}
g_1 &:= X, \\
g_2 &:= Y, \\
g_3 &:= [X,Y], \\
g_4 &:= [[X,Y],X], \\
g_5 &:= [[X,Y],Y],
\end{aligned}
$$

then generally the condition reads

$$
\frac{\partial}{\partial y_i}\Big|_p = g_i(p), \ \ i = 1, \ldots, 5
$$

where $p \in M$. Note that set (y_i) is then called an adapted frame at p.

Note that we keep the notation of the transformed controlling vector fields to be g_i and, if needed, we use the notation $g_i(z)$ to denote the vector fields transformed into $(z_1, z_2, z_3, z_4, z_5)$ coordinate system etc.

Next step of the Bellaïche's algorithm is the following: For $j = 1, \ldots, 5$ set

$$
z_j = y_j - \sum_{k=2}^{w_j-1} h_k(y_1, \ldots, y_{j-1}), \tag{4}
$$

where, for $k = 2, \ldots, w_j - 1$,

$$
h_k(y_1, \ldots, y_{j-1}) = \sum_{\substack{|\alpha|=k \\ w(\alpha)<w_j}} g_1^{\alpha_1} \ldots g_{j-1}^{\alpha_{j-1}} \left(y_j - \sum_{q=2}^{k-1} h_q(y) \right)(p) \frac{y_1^{\alpha_1}}{\alpha_1!} \cdots \frac{y_{j-1}^{\alpha_{j-1}}}{\alpha_{j-1}!}.
$$

Note that the choice of the polynomials h_k in (4) guarantees that the non–holonomic derivatives of z_j at p up to order $w_j - 1$ vanish. Clearly, only the

coordinates of the order 3, i.e. z_4 and z_5 will be different from the adapted coordinates y_4 and y_5, the lower order coordinates remain unchanged. Note that this step is employed due to the depth of the filtration (2,3,5) while for e.g. the trident snake robot, [3], with the filtration (3,6) this step is omitted. In our case,

$$z_4 = y_4 + 3y_1y_2 + (1/2)\sqrt{3}y_1^2 - (5/2)\sqrt{3}y_2^2,$$
$$z_5 = y_5 - 12y_1y_2 + \sqrt{3}y_1^2 + 5\sqrt{3}y_2^2.$$

Proposition 1. *The coordinates $(z_1, z_2, z_3, z_4, z_5)$ form the system of privileged coordinates.*

For general proof see [4].

Vector fields g_i are of order ≥ -1 and thus generally their Taylor expansion is of the form:

$$g_i(z) \sim \sum_{\alpha,j} a_{\alpha,j} z^\alpha \partial_{z_j},$$

where $\alpha = (\alpha_1, ..., \alpha_n)$ is a multiindex. Furthermore, if we define a weighted degree of the monomial $z^\alpha = z_1^{\alpha_1} \cdots z_n^{\alpha_n}$ to be $w(\alpha) = w_1\alpha_1 + \cdots w_n\alpha_n$, then $w(\alpha) \geq w_j - 1$ if $a_{\alpha,j} \neq 0$. Furthermore, the weighted degree of the monomial vector field $z^\alpha \partial_{z_j}$ is $w(\alpha) - w_j$. Recall that $w_j = \mathrm{ord}_p(z_j)$ from Definition 4 and in our particular case the coordinate weights are $(1, 1, 2, 3, 3)$. Grouping together the monomial vector fields of the same weighted degree we express $g_i, i = 1, 2$ as a series

$$g_i = g_i^{(-1)} + g_i^{(0)} + g_i^{(1)} + \cdots,$$

where $g_i^{(s)}$ is a homogeneous vector field of degree s. Note that this means that the controlling vector fields coefficients of ∂_{z_1} and ∂_{z_2} are formed by constants, the coefficients of ∂_{z_3} are linear in z_1 and z_2 and independent of the rest, and finally, the coefficients of ∂_{z_4} and ∂_{z_5} are formed by polynomials of the weighted degree 2, i.e. quadratic in ∂_{z_1} and ∂_{z_2} and linear in ∂_{z_3}. This fully corresponds to the fact that the weights of the coordinates are (1,1,2,3,3), see Section 2 for explanation. Then the following proposition holds, [4]:

Proposition 2. *Set $\hat{g}_i = g_i^{(-1)}, i = 1, 2$. The family of vector fields $(\hat{g}_1, \hat{g}_2)$ is a first order approximation of (g_1, g_2) at 0 and generates a nilpotent Lie algebra of step $r = 2$, i.e. all brackets of length greater than 2 are zero.*

The proof is just a straightforward computation of Lie brackets and is obvious. Because of its very extensive form we show the coordinate form of the approximated vector field corresponding to X only and we denote it by $\hat{X}$. Note that it is expressed in the original coordinate system $(x, y, \theta, \Phi_1, \Phi_2)$.

$$\hat{X} =$$

$$\partial_x$$

$$- \frac{1}{2(3\sqrt{3} - 2)^2} \Big(621\sqrt{3}x^2 - 13832\sqrt{3}xy - 12705\sqrt{3}y^2 + 120\sqrt{3}\Phi_1 + 24\sqrt{3}\Phi_2$$

$$- 186\sqrt{3}x + 264\sqrt{3}y + 360\sqrt{3}\theta + 644x^2 + 21626xy + 21580y^2$$

$$- 310\Phi_1 - 62\Phi_2 + 216x - 682y - 930\theta \Big)\partial_\theta$$

$$- \frac{1}{(3\sqrt{3} - 2)^3} \Big(-1164\sqrt{3}x^2 - 149430\sqrt{3}xy - 145220\sqrt{3}y^2 + 1755\sqrt{3}\Phi_1$$

$$+ 351\sqrt{3}\Phi_2 - 1700\sqrt{3}x + 4212\sqrt{3}y + 5265\sqrt{3}\theta - 7044x^2 + 272028xy$$

$$+ 252600y^2 - 170\sqrt{3} - 2550\Phi_1 - 510\Phi_2 + 3510x - 6120y - 7650\theta + 351 \Big)\partial_{\Phi_1}$$

$$- \frac{1}{2(3\sqrt{3} - 2)^3} \Big(1290\sqrt{3}x^2 + 106170\sqrt{3}xy + 99950\sqrt{3}y^2 - 680\sqrt{3}x + 5925x^2$$

$$- 204180xy - 163425y^2 + 680\sqrt{3} + 1404x - 1404 \Big)\partial_{\Phi_2}$$

The motion planning algorithm is similar to the one proposed in Section 3, i.e. it is sequential with periodic input (3) applied for the bracket motions. Note that according to [6], the periodic input (3) in nilpotent approximation can be applied to model the Lie bracket motions.

5   Global control

A well–known mathematical description of lateral undulation was presented by Hirose in 1993 based on empirical studies of biological snakes. Hirose discovered that a close approximation to the shape of a biological snake during lateral undulation is given by a planar curve whose curvature varies sinusoidally, more precisely $\varkappa(s) = |ab\sin(bs) - c|$, see [5]. Hirose named it a serpenoid curve and described it by

$$\begin{aligned} x(s) &= \int_0^s \cos(a\cos(b\sigma) + c\sigma)\mathrm{d}\sigma, \\ y(s) &= \int_0^s \sin(a\cos(b\sigma) + c\sigma)\mathrm{d}\sigma \end{aligned}$$

where $(x(s), y(s))$ are the coordinates of the point along the curve at arc length s from the origin and a, b, c are positive scalars. The following pictures within Figure 3 show the form of a serpenoid curve for different choices of parameters.

Furthermore, it was shown by Sainto in 2002 that a serpenoid curve of arc length 1 can be approximated by N identical discrete segments by calculating the angle Φ_i of segment $i \in \{1, ..., N\}$ with respect to the x axis according to $\Phi_i = a\cos\left(\frac{ib}{N}\right)$. This

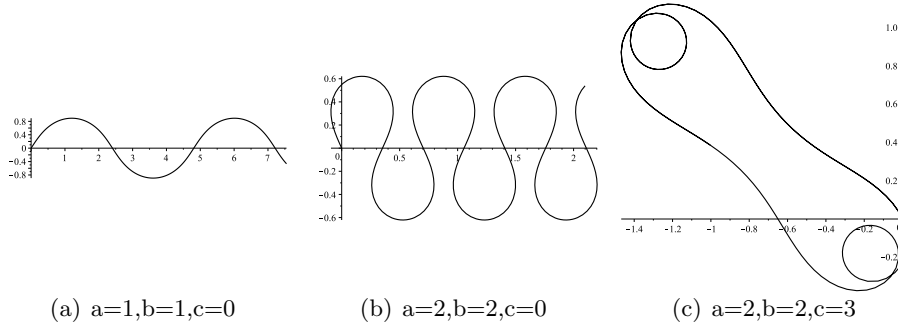(a) a=1,b=1,c=0   (b) a=2,b=2,c=0   (c) a=2,b=2,c=3

Figure 3. Serpenoid curves

implies that a snake robot with N identical discrete links attains a discrete approximation to the serpenoid curve by moving its link angles sinusoidally with a constant phase shift between the links. The pattern for lateral undulation is achieved by moving the joints of a planar snake robot according to

$$\Phi_i = A\sin(\omega t + (i-1)\delta) + \Phi_0, \tag{5}$$

where in our case, $i = 1, 2$, the offset $\Phi_0 = 0$ and only the amplitude A and frequency ω remain, see [5]. To use this model, we have to reparametrize the robotic system in such way that instead of controlling vector fields (1) and (2) parametrized by $\dot{x}$ and $\dot{y}$, we use vector field parametrized by $\dot{\Phi}_1$ and $\dot{\Phi}_2$. Then we use (5) as an input. Figure 4 shows the trajectory of a head point within one second.
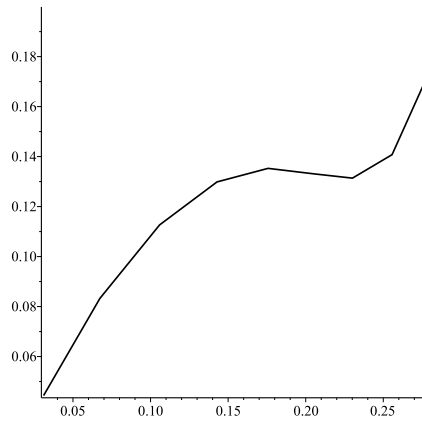

Figure 4. Head point trajectory

Finally, to demonstrate the similarity of the nilpotent approximation with the original controlling model see Figure 5. Note that due to locality property of the nilpotent approximation the time for comparison was decreased to 0,25 second.
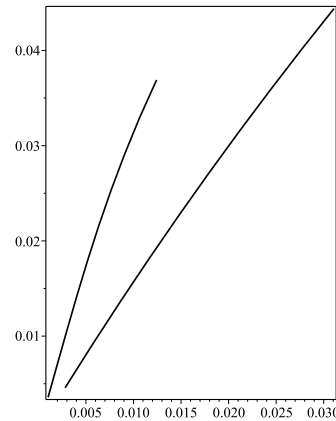
Figure 5. Nilpotent approximation comparison

6   Conclusion

We presented three possible models of a 3–link snake robot control, two of them local and one global. Note that if the motion is realized on a smooth surface with no obstacles then the control the robot is realized by the global control model. If the obstacles and narrow places are added such that the number of actually operational motorized joints decreases under the critical value of 4 then the local control takes place. We conclude that the questions of optimality are yet to be solved.

References

[1] Hrdina, J., Návrat, A., Vašík, P., Matoušek, R.: *CGA-based robotic snake control*, Adv.Appl. Clifford Algebr. (in print), 1–12 online (2016).

[2] Hrdina, J., Návrat, A., Vašík, P.: *Control of 3–link robotic snake based on conformal geometric algebra*, Adv.Appl. Clifford Algebr. **26**, n. 3, 1069–1080.

[3] Hrdina, J., Návrat, A., Vašík, P.: *Nilpotent approximation of a trident snake robot controlling distribution*, arXiv:1607.08500.

[4] Jean, F.: *Control of Nonholonomic Systems: From Sub–Riemannian Geometry to Motion Planning*, SpringerBriefs in Mathematics, Springer, 2014.

[5] Liljebäck, P., Pettersen, K.J., Stavdahl, Ø., Gravdahl, J.T., *Snake Robots, Modelling, Mechatronics and Control*, Springer, Advances in Industrial Control, 2013

[6] Murray, R.M., Zexiang, L., Sastry, S.S.: *A Mathematical Introduction to Robotic Manipulation*, CRC Press, 1994.

[7] Selig, J.M.: *Geometric Fundamentals of Robotics*, Springer, Monographs in Computer Science, 2004.